Sensors and Actuators A 220 (2014) 53–61

Contents lists available at ScienceDirect

Sensors and Actuators A: Physical

journal homepage: www.elsevier.com/locate/sna

Development of a novel ozone gas sensor based on sol–gel fabricated photonic crystal

M. Rahmat[a,b,*], W. Maulina[a], Isnaeni[c], D.Y.N. Miftah[a], N. Sukmawati[a], E. Rustami[a], M. Azis[a], K.B. Seminar[b], A.S. Yuwono[d], Y.H. Cho[c], H. Alatas[a]

[a] Department of Physics, Faculty of Mathematics and Natural Sciences, Bogor Agricultural University, Kampus IPB Darmaga, Bogor, West Java 16680, Indonesia

[b] Department of Mechanical and Biosystem Engineering, Faculty of Agricultural Technology, Bogor Agricultural University, Kampus IPB Darmaga, Bogor, West Java 16680, Indonesia

[c] Department of Physics, Graduate School of Nanoscience & Technology (WCU), KAIST Center for LED Research, and KI for the NanoCentury, KAIST, Daejeon 305-701, Republic of Korea

[d] Department of Civil and Environmental Engineering, Faculty of Agricultural Technology, Bogor Agricultural University, Kampus IPB Darmaga, Bogor, West Java 16680, Indonesia

ARTICLE INFO

Article history:
Received 10 February 2014
Received in revised form 27 August 2014
Accepted 2 September 2014
Available online 26 September 2014

Keywords:
Ozone gas
Photonic crystal sensor
Sol–gel method
Beer–Lambert effect

ABSTRACT

We have developed a novel ozone gas sensor based on one dimensional photonic crystal with two defects. In this platform, the gas is dissolved in a specific neutral buffer kalium iodide reagent to include the Beer Lambert effect. The corresponding photonic crystal which was fabricated by using sol–gel method consists of a high refractive index layer of TiO_2 and a low refractive index layer of SiO_2. Prior to the fabrication of corresponding photonic crystal, we grew the TiO_2 and SiO_2 single layer separately in order to ensure that the performance of each layer fulfilled the required characteristics provided by our simulation. After that, the fabrication processed was conducted layer-by-layer and inspected by spectrophotometer. The performance test of the fabricated photonic crystal, including its validation, accuracy and sensitivity, was then conducted through spectroscopic treatment and we used ozonizer as the gas source. Validation test was performed by comparing the results with measurement using NBKI method and showed a good agreement. It was found that the accuracy value is up to 98.75%. Based on a statistical approach, we found that the limit of detection is 1.067 $\mu g/m^3$ ambient air.

1. Introduction

It has been widely known that ozone (O_3) pollution cannot only affect human health, but also damage some types of plants. Under long time exposure, 0.3 ppm low ozone concentration can cause irritation, while the higher level ~9.0 ppm may lead to edema pulmonary. Moreover, at least there are 57 species of plants that are susceptible to ozone gas. The ozone gas diffuses via stomata and terminates palisade cell to form brownish yellow spot. In the case of tobacco plant, for 4 h exposure of 0.08–0.10 ppm concentration results in serious damage [1,2].

One of the standard measurements of ozone gas concentration provided by the International Ozone Association (IOA, Standarization Committee 001/87) is neutral buffer potassium iodide (NBKI) method. The NBKI solution consists of potassium iodide (KI), disodium hydrogen phosphate dodecahydrate ($Na_2HPO_4{\cdot}2H_2O$), and potassium dihydrogen phosphate (KH_2PO_4). This method is based on oxidation of iodide ion to form iodine ozone when the related ozone is bubbled through a solution of NBKI. The main advantage of this method is its reproducibility when conducted under strict conditions of a particular sampling technique, reaction time and ozone gas flow rate [3].

Over the past years, ozone sensors have been developed based on various platforms such as In_2O_3 nano-crystals [4], WO_3 [5], electrochemical cell [6,7], enzyme-based biosensor [8], ZnO nanorod [9], chemo luminescent [10], and optical sensors [11,12]. Several types of optical sensors that have been developed were based on photonic crystals [13], fiber optics [14] and hybrid plasmonic photonic crystals [15]. Regarding the photonic crystal sensor, it has even been reported to allow high sensitivity for the detection limit

* Corresponding author at: Department of Physics, Faculty of Mathematics and Natural Sciences, Bogor Agricultural University, Kampus IPB Darmaga, Bogor, West Java 16680, Indonesia. Tel.: +62 2518625728; fax: +62 2518625728.
E-mail addresses: m.rahmat@ipb.ac.id, rahmat32@gmail.com (M. Rahmat), alatas@ipb.ac.id (H. Alatas).

http://dx.doi.org/10.1016/j.sna.2014.09.020
0924-4247/

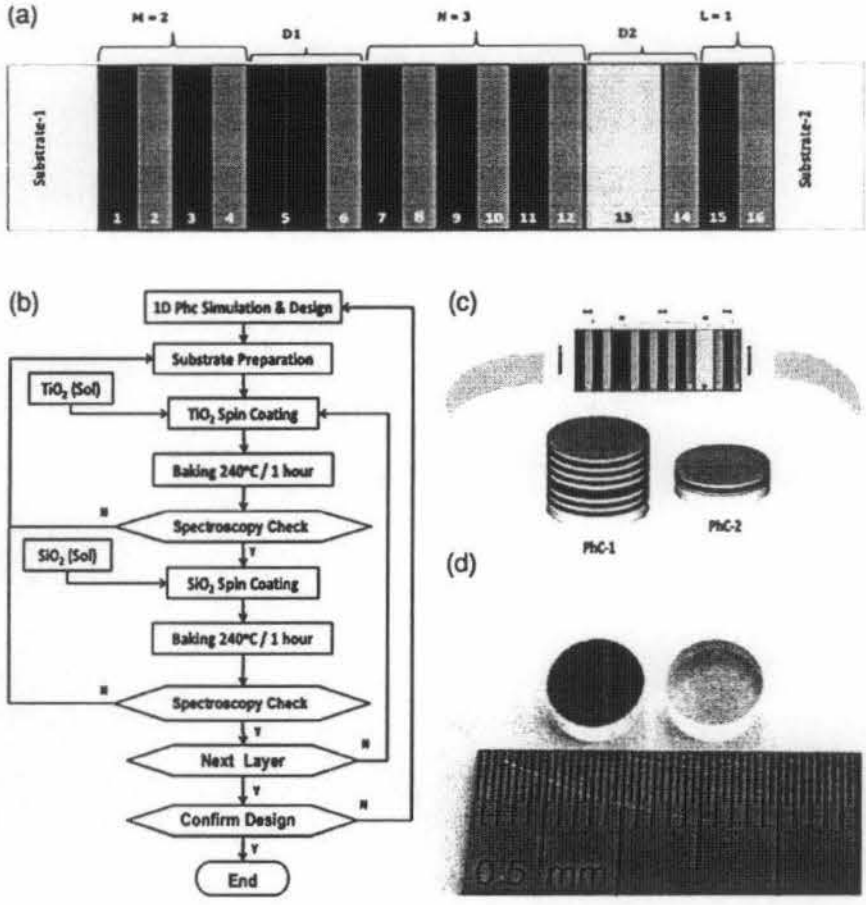

Fig. 1. (a) 1D-PhC model for ozone gas sensor. (b) Flow process of 1D-PhC fabrication. (c) Illustration of deposition coating of PhC-1 and PhC-2. (d) Photograph of sol–gel fabricated PhC-1 (left) and PhC-2 (right).

up to order of sub-pg/mL [16]. The application of one dimensional photonic crystal (1D-PhC) with two defects for detecting NO_2 gas has also been carried out in an integrated gas monitoring system [17]. It has widely been discussed that the presence of defects in a periodic optical structure leads to the existence of photonic pass band (PPB) inside the photonic band gap (PBG) [18]. Each of two defects functions as a regulator and receptor. The regulator layer which was designed permanently to set the fixed PPB has optical thickness two times greater than the regular layer, while the receptor layer was designed to place the analyte.

In our recent work, we have successfully developed a 1D-PhC based ozone sensor which was fabricated using sol–gel method. The basic principle of this sensor is the application of photonic pass band (PPB) variation due to refractive index changes of the receptor enhanced by the Beer-Lambert effect in NBKI method. This article will explain the result of the performance of the sensor.

2. Design and simulation of 1D-PhC

We considered a 1D-PhC structure consisting of two or more periodic transparent dielectric materials with different refractive indices, while the optical thickness of each layer is set to be a quarter of operational wavelength [19,20]. When lights pass through the layers, each layer partially reflects the corresponding light. The Bragg reflection creates when constructive interference between forward and backward propagating lights leads to a strong reflectance. This reflection is responsible for the occurrence of photonic band gap (PBG) where for certain wavelength interval light cannot be propagated [21]. Remarkably, when a defect is introduced to this periodic system by modifying one or more layers optical path in the structure it bring about the existence of photonic pass band (PPB) that allows light to propagate in a narrow interval inside the corresponding PBG. In principle, the insertion of two defects in 1D-PhC can generate PPB with unique characteristics with respect to the material changes on defect layers. The change of optical path of the first defect leads to the shift of PPB peak, while the one on the second defect layer causes the change of PBB peak value. It is this later characteristic that can be used as sensing platform [18].

We design a 1D-PhC comprising alternating two different dielectric materials and two defects in the following arrangement:

$$(n_s)\left(\frac{n_h}{n_l}\right)^M D_1 \left(\frac{n_h}{n_l}\right)^N D_2 \left(\frac{n_h}{n_l}\right)^L (n_s) \quad (1)$$

As shown in Fig. 1a. The symbol (n_h/n_l) denotes one unit cell where n_h and n_l represent layers of high and low refractive indices with the associated thicknesses are d_h and d_l, respectively, while n_s represents substrate. The symbols D_1 and D_2 are related to regulator and receptor defect cell, respectively, where $D_1 \equiv (n_{reg}/n_l)$ and $D_2 \equiv (n_{rec}/n_l)$. The corresponding thicknesses of both defects n_{reg} and n_{rec} layers are d_{reg} and d_{rec}, respectively. The numbers of cells in each segment are represented by M, N, L and we considered M = 2, N = 3 and L = 1., respectively. This design is based on optimum configuration where N = M + L [17]. For substrate layer we used quartz crystal with refractive index of 1.544, SiO_2 as low index layer with refractive index of 1.45, and TiO_2 with refractive index of 2.21 as high index layer as well as regulator layer. In this case, light

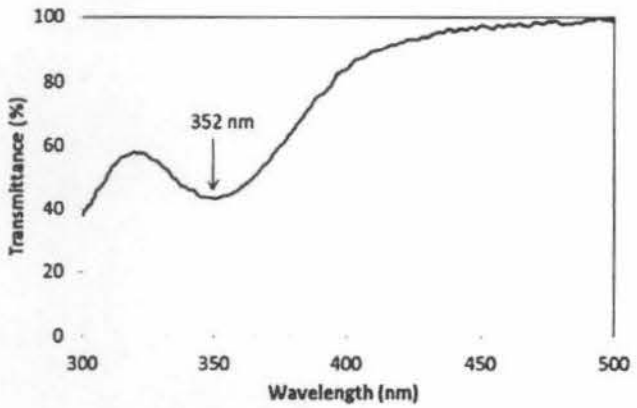

Fig. 2. Absorption spectra of ozone absorbed in NBKI.

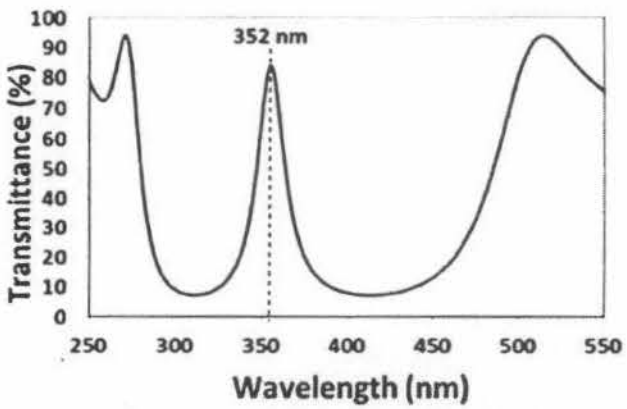

Fig. 3. Simulation result of PPB spectrum characteristic.

propagates from substrate-1 through the 1D-PhC and is detected after substrate-2.

As mentioned previously, this sensor is not only developed based on the principle of PPB variation, but also by employing the electromagnetic absorption of material known as Beer-Lambert effect. Therefore, firstly we have to determine the analyte absorption wavelength. For this purpose, we poured 10 ml NBKI solution into an impinger tube added by ozone gas obtained from ozonizer at rate of 0.4 l/min for 15 min. To obtain the spectrum characteristics of ozone dissolved in NBKI solution (Fig. 2) we used an Ocean Optics USB 4000 spectrophotometer. The magnitude of absorption is presented by minimum transmittance where its corresponding wavelength is considered as operational wavelength (λ_0). The measurement result showed that the average magnitude of absorption is 351.58 ± 3.53 nm. To simplify, we take the value of 352 nm.

To design the corresponding 1D-PhC, we conducted a simulation by means of transfer matrix method (TMM) [18]. The structure (1) was set to satisfy the quarter-wave optical thickness (QWOT) condition, in which $n_h d_h = n_l d_l = \lambda_0/4$, where λ_0 is the operational wavelength. The optical thickness $n_{reg}d_{reg}$ was fixed to $\lambda_0/2$. Here, the physical thickness of high and low index layers were set to $d_h = 39.82$ nm and $d_l = 60.69$ nm, respectively. These chosen values satisfy the aforementioned QWOT condition with $\lambda_0 = 352$ nm. In the mean time, the thickness of regulator and receptor layers were set to $d_{reg} = 79.64$ nm and $d_{rec} = 1$ mm, respectively, while $n_{reg} = n_{rec} = 2.21$. The simulation result is presented in Fig. 3 showing the existence of PPB with the corresponding peak is at 352 nm. Clearly, this wavelength is coincides with the lowest transmittance of ozone-dissolved NBKI as shown in Fig. 2 to accommodate the Beer-Lambert effect.

To examine the response behavior of the corresponding 1D-PhC, we also performed another simulation by assuming the n_{rec} to be in the range of 1 to 2. The objective of this wide range refractive index is to predict the change of analyte refractive index which was assumed to be inside it. The simulation results are shown in Fig. 4a for PPB spectrum changes with respect to the refractive index, and Fig. 4b showing the correlation plot between refractive index and the peak of PPB.

3. Fabrication process

To fabricate the corresponding 1D-PhC that consisting of TiO_2 and SiO_2 materials, we choose the sol–gel method. This method is a wet-chemical technique which is commonly used for manufacturing glass and ceramic materials [22]. In this process, the reaction of sol (or solution) forms a gel-like tissue which contains a liquid and solid phase.

Generally, the precursors for this process are alkoxides metal or metal salt where under hydrolysis reaction and polycondensation form colloid. The basic structure or morphology of solid phase can vary from discrete colloid particle to polymer tissue chain [23–25]. Some of the advantages of sol–gel method are its capability to form a good adhesion of thin-layer with the substrate and easiness to form complex geometry, even in a gel state. This sol–gel process can produce high purity products because the organic-metal precursor obtained from ceramic oxide can be mixed, diluted in specific solution and hydrolyzed into sol. Moreover, the gel composition and process condition can also be controlled. Likewise, this method is considered simple, cheap and effective to produce high quality coating and also can be conducted in low sintering temperature (200–600 °C) [25,26].

For TiO_2 precursor, we used titanium isopropoxide (TIP), ethanol (C_2H_5OH) and acetic acid (CH_3COOH), while the SiO_2

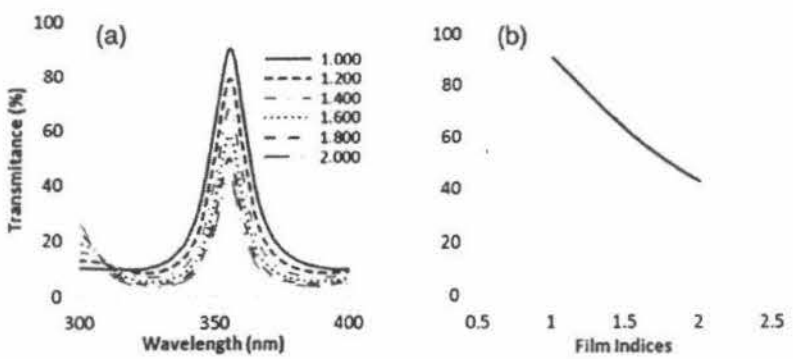

Fig. 4. Simulation result of refractive index at second defect, (a) PPB spectrum characteristic on each refractive index, (b) correlation between refractive index change towards the peak of PPB transmittance.

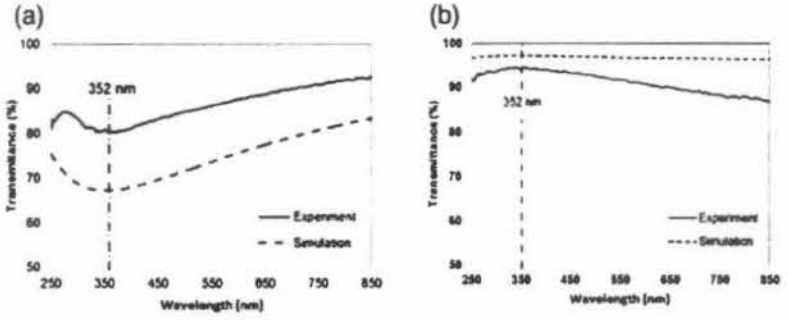

Fig. 5. (a) TiO_2 film thickness at different spin coating speed 4000 rpm (left panel) 5000 rpm (mid panel) and 6000 rpm (right panel). (b) The effect of solvent variation.

precursor was made using tetraorthosilicate (TEOS), ethanol (C_2H_5OH), hydrochloric acid (HCl) and distilled water (H_2O). All main precursor materials are from Sigma–Aldrich.

To fabricate the corresponding 1D-PhC, we first grew the single layers of both TiO_2 and SiO_2 separately. This step is taken in order to determine the optical path satisfying a QWOT condition of each layer so as to obtain the fabrication parameters (e.g. spinning speed and time, sol–gel composition) that ensure the quality of the layer and position of the considered PPB peak at 352 nm. The corresponding physical and morphological characteristics of those single layers were tested using scanning electron microscope (SEM), Hitachi S-4800, while the optical performances were tested using UV-VIS Ocean Optics USB 4000 and High-sensitivity Maya 2000Pro spectrometers. The following are the detailed processes in synthesizing the corresponding single layers and 1D-PhC.

3.1. Synthesis of TiO_2 and SiO_2 single layer

The TiO_2 single layer was deposited on a quartz crystal substrate. A solution composed of ethanol 1500 ml and acetic acid 200 ml was mixed and stirred for 5 min at 800 rpm and then titanium isopropoxide (TIP) 125 ml was added into the solution and we re-stirred for 5 min at 800 rpm. Afterward, the corresponding TiO_2 solution was dripped evenly onto substrate. The coating process was then performed for 60 s at 6000 rpm. After that, sample was heated on furnace for 1 h at 240 °C and then cooled at room temperature. To characterize the result, we used SEM and spectrophotometer. Based on spectroscopy characterization the transmittance of this single layer is given in Fig. 5a, showing that the lowest transmittance is at 352 nm. The lowest trasmittance was obtained by optimizing the spin coating duration and speed as well as the amount of solvent.

The example of TiO_2 layer thickness optimization process with respect to spin coating speed variations are given in Fig. 6a, while the variations of transmittance characteristics with respect to different amount of solvent are given in Fig. 6b showing the wavelength shift of minimum transmittance.

Similar to TiO_2, the SiO_2 layer was also deposited on quartz crystal substrate. A solution composed of ethanol 1600 μl ethanol, 39 μl H_2O and 30 μl HCl were mixed and stirred at 800 rpm for 5 min, and then 90 μl TEOS was added into solution and re-stirred at 800 rpm for 5 min. The SiO_2 solution was also dripped evenly onto substrate. The spin coating process was performed for 60 s at 6000 rpm. Afterward the sample was furnaced for 1 h at 240 °C and then cooled at room temperature. We finally characterized it by using SEM and spectrophotometer. The transmittance of this SiO_2 layer is depicted in Fig. 5b, showing that the highest transmittance is at 352 nm.

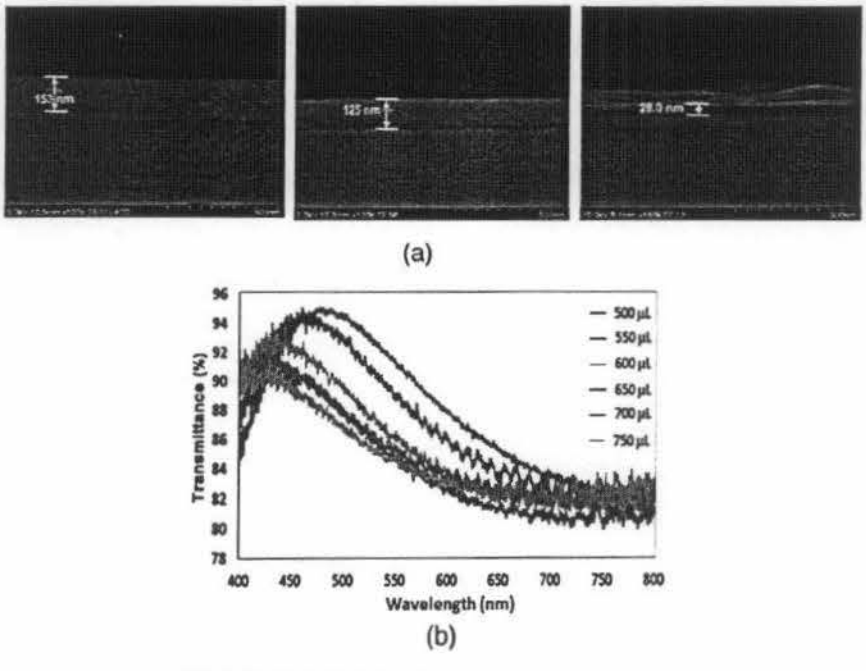

Fig. 6. Spectrum characteristic of single (a) TiO_2 (b) SiO_2 layer.

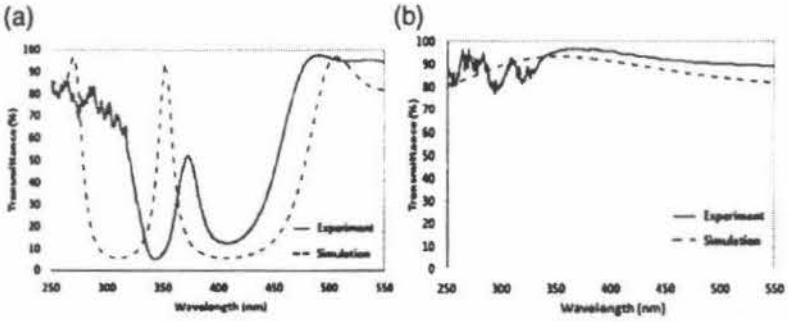

Fig. 7. Spectrum characteristics of fabricated (a) PhC-1 and (b) PhC-2.

It is important to note that the opposite transmittance characteristic between TiO_2 and SiO_2 is due to the contrast between the associated layers and the substrate. Here, the refractive index of TiO_2 is higher than substrate, whereas the SiO_2 is lower. In the mean time, we did not measure the precise thickness of each TiO_2 and SiO_2. However, based on our simulation results their thicknesses are 39.82 and 60.69 nm, respectively. Detailed discussion about these results will be further elaborated in the next section.

3.2. Synthesis of 1D-PhC

The deposition flow process to construct the corresponding 1D-PhC was carried out in two steps. The first one is to create 12 layers started from the 1st up to 12th layer which was implemented on the quartz crystal substrate-1. These 12 layers 1D-PhC is denoted as PhC-1. This process also included the first defect layer which was placed at the 5th layer. Deposition flow process for each layer is given in Fig. 1b. The second deposition process created three layers, started from 16th down to 14th layer implemented on the second quartz crystal substrate, while the 13th layer was set to be filled by analyte solution. We denote these 3 1D-PhC layers as PhC-2. Illustration of these two separated 1D-PhC's is shown in Fig. 1c.

To ensure the conformity between the manufacturing process, predefined design and simulation, a spectroscopy test was performed at each deposition layer to provide feedback to the fabrication process and the design plan. Therefore, it can be used as a guidance in subsequent process and provides information to analyze the sample performance at each step and its repeatability.

Based on the measurement result on N-M-L of 2-3-1 pattern, it was found that the associated PPB transmittance spectrum was in the range of UV wavelength, reaching its with peak at 375 nm. Compared to the simulation result which showed 352 nm, it is shown that the deviation is only 7%. This deviation is still tolerable since the absorption wavelength of ozone dissolved NBKI is in the range of 320–400 nm (see Fig. 2). Therefore, the precise value of refractive indices as well as thicknesses of both fabricated TiO_2 and SiO_2 layers are not necessary to be examined.

It is worth noting, however, the fabrication process was inspected by spectroscopy method which characterized the change of transmittance spectrum on each layer. This result was further compared with the one generated by simulation (see Fig. 7). Fig. 7a shows the PBB spectrum occurred at PhC-1 which composed of 12 layers including the first defect set at 5th layer, while Fig. 7b shows the spectroscopic analysis occurred at PhC-2 which has 3 layers (SiO_2-TiO_2-SiO_2). To examine the accuracy in each fabricated layer, we analyzed the transmittance using spectroscopy every time we added one layer by comparing it with our simulation (see Fig. 1b). It was found that both fabrication of PhC-1 and PhC-2 are in good agreement with the simulation results.

The result on Fig. 7 reveals that PBG bandwidth is smaller than the simulation results while the PPB's peak position is shifted. This happens because the actual refractive index contrast between high and low indices of the fabricated 1D-PhC is smaller and their thicknesses are not the same as that used in the simulation. Since, we have to avoid the layer crack, we found that the optimal baking temperature is at 240 °C. Therefore, it is obvious that this fabrication process could not achieve the simulation value of the refractive index of each material. One of the difficulties encountered in the sol–gel method is the absence of control of layer thickness and refractive index, thus allowing deviation in the consistency of the results of the synthesis of each layer. Fig. 7a shows the deviation of the wavelength reaching 375 nm PPB. Fortunately, this wavelength is still in the range of absorption spectra of absorbed ozone in NBKI solution around 325–400 nm.

Fig. 1d shows the sol–gel fabricated 1D-PhC. The photonic crystal was made on quartz crystal substrate with a diameter of 6.5 mm. This diameter size is set to fit the impinger design that will be used in sensing test. The picture on the left side is the PhC-1. Violet color indicates the presence of a reflection in the 325–400 nm bandwidth, whereas the right picture is PhC-2 which is more transparent than PhC-1 due to less number of layers.

4. Performance test

Performance test of the 1D-PhC sensor in detecting the ozone was conducted in several steps: (i) preparing of ozone sample in insulation chamber, (ii) dissolving the ozone in NBKI analyte, (iii) characterizing the spectroscopy spectrum of the sample under different levels of concentration, and (iv) performing the real time performance test. The test was conducted by following the characterization schemes shown in Fig. 8. It was carried out through modifying conventional impinger equipped with 1D-PhC sensor inside.

It should be emphasized that we did not deal with the repeatability of the corresponding test in the following discussion since the robustness of the sol–gel fabricated 1D-PhC and its fabrication repeatability as discussed in the previous section are good enough to guarantee repeatable measurement results.

The next step, ozone sample was prepared in insulation chamber to obtain the desired gas composition. Insulation chamber was cleaned away from the gas before the ozone gas sample filled into the chamber. Such initial condition showed that the chamber had equal pressure with outside air pressure, which was shown by a zero value on the pressure gauge. The first step that must be taken to clean the chamber is closing all valves (see Fig. 8) of the chamber except those that connect to either the vacuum pump or N_2 gas cylinder. Gas inside the insulation chamber was sucked out using a vacuum pump to obtain the insulation pressure of −80 kPa while the N_2 valve was closed. After this, we closed the valve of vacuum pump and open the N_2 valve so that the pressure reached ~0 kPa. The purpose of this process is to remove all gasses inside the chamber and only N_2 that remained inside the chamber. This process

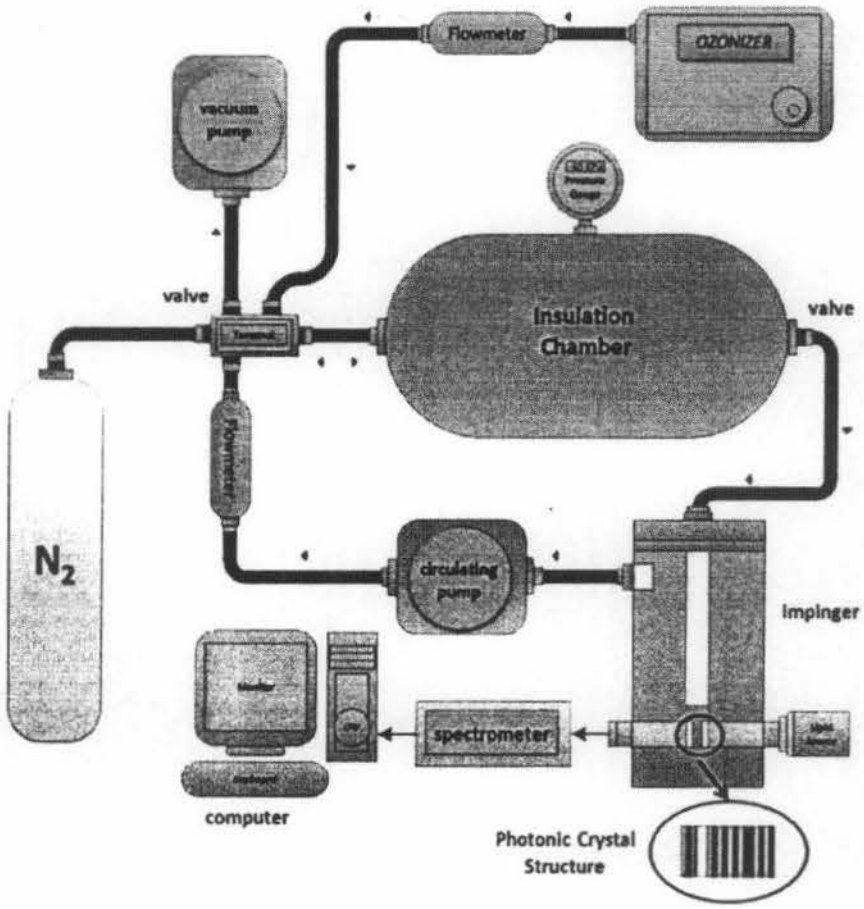

Fig. 8. Schematic diagram of 1D-PhC characterization for ozone detection

was performed in two or three times in order to ensure that the chamber condition was clean.

The filling of ozone into insulation chamber was carried out by re-sucking the N_2 from the insulation chamber until −40 kPa and then filled with ozone to reach ~0 kPa. The ozone gas was filled using ozonizer at 2 l/min. After completing this process, the ozone sample was ready to be used in the further step.

In the next step we dissolved ozone in NBKI solution. First, we closed the valve leading to N_2 gas, vacuum pump and ozonizer. Then, we opened the valve leading to circulating pump and impinger. The circulating pump was turned on to generate close circulation, namely the gas from insulating chamber leads to impinger, circulating pump, flow meter and back to insulating chamber. Ozone was absorbed by NBKI solution in impinger containing 10 ml NBKI solution. Circulation process occurred for 30 min with 0.4 l/min flow meter rate. The analyte as the result of reaction between ozone and NBKI solution was ready for further analysis.

Analysis of the analyte was conducted by dividing 10 ml analyte into two parts. A total of 5 ml was analyzed by NBKI method to determine the ozone concentration in NBKI solution, while the other 5 ml was used to test the 1D-PhC sensor under different levels of concentration. The concentration value obtained from NBKI analysis was considered as the reference in testing sensor performance based on spectroscopy analysis. Dissolved ozone concentration in NBKI solution (μg per ml solution) was converted into μg per m^3 of ambient air by calculating the flow rate, absorption time, temperature, pressure, and environment humidity during the process.

By using pre-determined analyte concentration, the measurement of sensor performance was conducted by spectrometer under different levels of concentration by adding a blank solution i.e. NBKI solution that did not react with ozone gas. The performance measurement was conducted in impinger connected to a light source and Ocean Optics USB 4000 spectrometer. Spectroscopy measurement was recorded continuously at every addition of 1 ml of blank solution.

Following this, the fabricated 1D-PhC was mounted on a modified impinger as shown in Fig. 9. The 1D-PhC were placed on the bottom of the impinger and submerged in NBKI reagents. The PhC-1 and PhC-2 is placed facing each other with a distance of about 1 mm and the gap is used as receptor chamber filled by NBKI solution. Afterward, the light source of LED with a wavelength of 375 nm is placed on the right hand side of PhC-1, according to the characteristics of PPB of fabricated 1D-PhC. Spectrophotometer detector was placed right after the PhC-2 to detect light transmission that passed through photonic crystal. When the circulation pump started, the gas containing ozone that flow to the solution will react with the NBKI solution [3]. Obviously, the amount of ozone that reacts with the corresponding NBKI solution increased in line with the length of the process. The change of the concentration affected the light transmittance where its variation was detected and measured by the spectrophotometer.

From this measurement, we have obtained the characteristics of the spectroscopy spectrum at each level of ozone gas absorbed in NBKI solution as given in Fig. 9a, while Fig. 9b represents the correlation curve between PPB's peak and various concentration levels. From the regression analysis of transmittance and concentration correlation curves we obtained a logarithmic equation: $T = -56.66 \ln C + 222.82$, where C is the concentration of ozone gas (μg/m^3) and T is the transmittance (%), with a

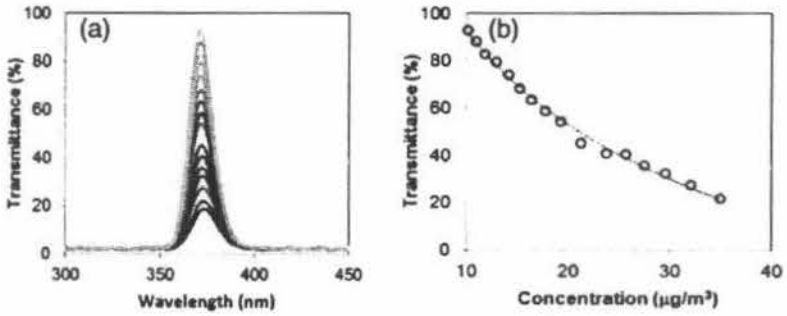

Fig. 9. Spectrum characteristics of ozone detection test results using 1D-PhC sensor. (a) Changes of PPB spectrum towards increasing concentration. (b) Correlation of PPB's peak towards ozone concentration

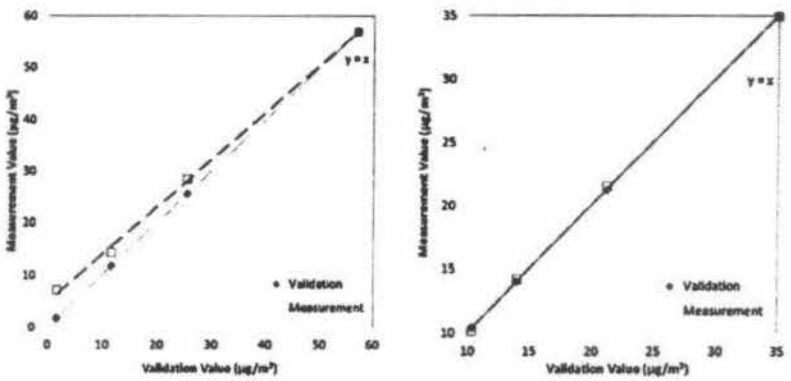

Fig. 10. Validation data of ozone measurement. (a) With and (b) without 1D-PhC sensor.

regression coefficient of 99.48%. The equation was used to calculate the value of concentration when the transmittance measurements were performed directly to the 1D-PhC structure.

The sensor testing for ozone detection was performed using the same procedure as shown in Fig. 8. Performance test was carried out in four steps i.e. (i) preparing the insulation chamber, (ii) cleaning the insulation, (iii) filling the ozone into the chamber and (iv) circulating the ozone in a closed loop. The transmittance measurement was carried out simultaneously with the ozone absorbing process during the fourth step. The spectroscopic and secondary data such as temperature, pressure and humidity were recorded every 2 min for 30 min.

The next performance test is to evaluate sensor accuracy and sensitivity. For comparison, impinger without 1D-PhC was tested in similar measurement method. In impinger, the related 1D-PhC was replaced by blank substrate quartz crystal. Therefore, the mechanism of the measurement was based on Beer-Lambert effect only, where light was absorbed by the analyte. The objective of this test is to compare the measurement results with and without 1D-PhC. Analyte sample preparation followed the same procedure, as illustrated by Fig. 8, to get analyte NBKI solution that reacted with ozone.

Similar to the early steps of the performance test, 10 ml analyte was divided into two parts, the first 5 ml was for NBKI analysis and the other 5 ml was used for testing the sensor performance. The value obtained from NBKI analysis result was used as a reference for sensor performance analysis. However, there was a slight difference in the testing procedure. Sensor performance analysis was conducted using spectroscopic method at every addition of 1 ml of blank solution. The addition was carried out in 5 times to obtain 10 ml analyte solution. From this 10 ml analyte sample, we took 5 ml to repeat NBKI analysis while the remaining 5 ml was treated under the same procedure to reach 10 ml again. With three replications, four data were obtained to validate the measurement results. A similar procedure was conducted to compare the system performance with and without 1D-PhC, but we only used substrate in the impinger for the measurement performance without 1D-PhC.

The obtained data of ozone concentration of with and without 1D-PhC cases are shown in Fig. 10a and b. Both figures show the results of spectroscopic measurements and validation curve from NBKI measurement. The straight line $y = x$ is a calibration line which indicates how close the value obtained from spectroscopic measurements to actual value. By comparing these two results, error value whics is calculated by mean average percentage error (MAPE) can be obtained. It was found that 1D-PhC has MAPE of 1.25%, while the one without 1D-PhC has MAPE of 26.29%. In other words, the case with 1D-PhC exhibits accuracy up to 98.75%, therefore it is more accurate than the one without 1D-PhC.

From the aforementioned process of dividing 10 ml analyte, we can also generate sensitivity curve as shown in Fig. 11. The curve shows correlation data between transmittance and logarithmic concentration. The 1D-PhC measurement has steeper gradient. The larger value of gradient absolute indicates more sensitivity. It could be found that gradient absolute value in measurement with and without 1D-PhC were 56.66 and 38.21, respectively. Clearly, this result shows that the use of 1D-PhC is more sensitive.

Fig. 11 also presents that natural characteristic of analyte in measurement without 1D-PhC could be detected using spectrophotometer as interaction of molecules with light in accordance with the Beer-Lambert effects. It occurs when the optical signal wavelength matches with natural wavelength of molecular energy level. The resonance wavelength depends on the number and weight of the atoms in the molecule, or equivalent to the amount and strength of its chemical bonds. If the chemical structure is more complex, the absorption characteristic of molecules is expressed in the specific range of vibration frequency. On the other hand, measurement

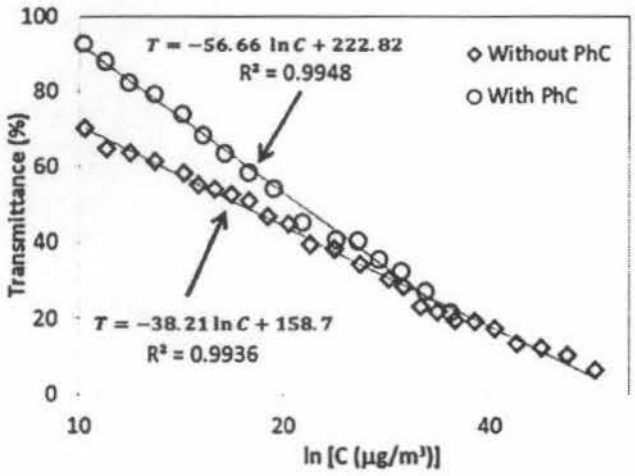

Fig. 11. Ozone concentration correlation curve obtained from measurement with and without 1D-PhC

using 1D-PhC had a greater gradient value which indicated that the presence of it could increase measurement sensitivity.

The increase of sensitivity is also due to the variation of PPB characteristics with respect to the variation of refractive index in the second defect that contains analyte. The reason underlying this is that increasing analyte concentration is in line with the increasing refractive index. In this reaction, the measurement using NBKI reagent only reacted with ozone gas, and there are no other gasses will react with the NBKI solution. Therefore, it ensures the sensor selectivity.

Another important parameter that should be examined is the limit of detection (LOD). This parameter can be calculated statistically using software provided by the University of Maryland [27]. Approximate value of LOD can be determined using formula LOD = 3.3(SD/S) where SD is the standard deviation between the measurement and validation data and S is the slope of the calibration line. The corresponding SD can be determined based on the standard deviation of y-intercept of regression line. It was found from the calibration line in Fig. 10b, that SD = 0.3248 and S = 1.0048; as a result the LOD is 1.067 µg/m^3 ambient air. Using the same procedure, we found that in the case without 1D-PhC the corresponding LOD is 2.838 µg/m^3 ambient air. Clearly, this fact re-emphasize that the case with 1D-PhC is much better than the one without 1D-PhC.

Finally, it is important to emphasize that the sensitivity of the 1D-PhC can be enhanced by increasing the refractive index contrast between high and low index layers [18]. Increasing the number of cells can be the other alternative that should be considered to adjust sensitivity, range of measurement and its LOD.

5. Conclusion

We have successfully developed a 1D-PhC sensor for ozone detection based on sol–gel method. The 1D-PhC model with 2-3-1 pattern using Beer-Lambert effect shows higher sensitivity compared to the conventional measurement. Moreover, measurement with 1D-PhC demonstrated good accuracy up to 98.75%. This study also proved that the existence of 1D-PhC can increase measurement sensitivity as a result of analyte refractive index changes in second defect that influence PPB response as demonstrated by its LOD value. The combination between Beer-Lambert effect and PPB phenomena improves the performance of corresponding sensor, especially sensitivity and selectivity of the sensor that allows its application in environmental and biological monitoring systems.

Acknowledgement

This work was funded by the Integrated Outstanding Scholarship Program from Ministry of Education and Culture, Republic of Indonesia, under contract no. 70811/A2.5/LN/2010. We would like to extend our thank to the Centre for Environmental Research – IPB (PPLH-IPB) that allowed us to use their facilities. We also thank to KAIST Nano-Bio-Photonics members who supported this research collaboration.

References

[1] M. Kampa, E. Castanas, Human health effects of air pollution, Environ. Pollut. 151 (2008) 362–367.
[2] M. Norval, A.P. Cullen, F.R. de Gruijl, J. Longstreth, Y. Takizawa, R.M. Lucas, F.P. Noonan, J.C. van der Leun, The effects on human health from stratospheric ozone depletion and its interactions with climate change, Photochem. Photobiol. Sci. 6 (2007) 232–251.
[3] K. Rakness, G. Gordon, B. Langlais, W. Masschelein, N. Matsumoto, Y. Richard, C.M. Robson, I. Somiya, Guideline for measurement of ozone concentration in the process gas from an ozone generator, Ozone 18 (1996) 209–229.
[4] A. Gurloa, M. Ivanovskayaa, N. Bârsanb, M. Schweizer-Berberichb, U. Weimarb, W. Göpelb, A. Diéguezc, Grain size control in nanocrystalline In_2O_3 semiconductor gas sensors, Sens. Actuators B 44 (1–3) (1997) 327–333.
[5] M. Bendahan, R. Boulmani, J.L. Seguin, K. Aguir, Characterization of ozone sensors based on WO_3 reactively sputtered films: influence of O_2 concentration in the sputtering gas, and working temperature, Sens. Actuators B 100 (3) (2004) 320–324.
[6] R. Knake, P.C. Hauser, Sensitive electrochemical detection of ozone, Anal. Chim. Acta 459 (2002) 199–207.
[7] B.J. Johnson, S.J. Oltmans, H. Vömel, Electrochemical concentration cell (ECC) ozonesonde pump efficiency measurements and tests on the sensitivity to ozone of buffered and unbuffered ECC sensor cathode solutions, J. Geophys. Res. 107 (D19) (2002) 4393.
[8] E. Bakker, Electrochemical sensors, Anal. Chem. 76 (2004) 3285–3298.
[9] F.S.-S. Chien, C.-R. Wang, Y.-L. Chan, H.-L. Lin, M.-H. Chen, R.-J. Wu, Fast-response ozone sensor with ZnO nanorods grown by chemical vapor deposition, Sens. Actuators B 144 (1) (2010) 120–125.
[10] V. Yushkov, A. Oulanovsky, N. Lechenuk, I. Roudakov, K. Arshinov, F. Tikhonov, L. Stefanutti, F. Ravegnani, U. Bonafè, T. Georgiadis, A chemiluminescent analyzer for stratospheric measurements of the ozone concentration (FOZAN), J. Atmos. Ocean. Technol. 16 (1999) 1345–1350.
[11] R.A. Potyrailo, S.E. Hobbs, G.M. Hieftje, Near-ultraviolet evanescent-wave absorption sensor based on a multimode optical fiber, Anal. Chem. 70 (8) (1998) 1639–1645, http://dx.doi.org/10.1021/ac970942v.
[12] S. O'Keeffe, C. Fitzpatrick, E. Lewis, An optical fibre based ultra violet and visible absorption spectroscopy system for ozone concentration monitoring, Sens. Actuators B 125 (2) (2007) 372–378.
[13] V.N. Konopsky, E.V. Alieva, Photonic crystal surface waves for optical biosensors, Anal. Chem. 79 (2007) 4729–4735.
[14] O.S. Wolfbeis, Fiber-optic chemical sensors and biosensors, Anal. Chem. 80 (2008) 4269–4283.
[15] X. Yu, L. Shi, D. Han, J. Zi, P.V. Braun, High quality factor metallodielectric hybrid plasmonic–photonic crystals, Adv. Funct. Mater. 20 (2010) 1–7.
[16] F. Liang, N. Clarke, P. Patel, M. Loncar, Q. Quan, Scalable photonic crystal chips for high sensitivity protein detection, Opt. Express 21 (2013) 32306–32312.
[17] M. Rahmat, W. Maulina, E. Rustami, M. Azis, D.R. Budiarti, K.B. Seminar, A.S. Yuwono, H. Alatas, Performance in real condition of photonic crystal sensor based NO_2 gas monitoring system, Atmos. Environ. 79 (2013) 480–485.
[18] H. Alatas, H. Mayditia, H. Hardhienata, A.A. Iskandar, M.O. Tjia, Single frequency refractive index sensor based on finite one-dimensional photonic crystal with two defects, Jpn. J. Appl. Phys. 45 (8B) (2006) pp. 6754.
[19] E. Yablonovitch, Inhibited spontaneous emission in solid-state physics and electronics, Phys. Rev. Lett. 58 (20) (1987).
[20] C. Sibilia, T.M. Benson, M. Marciniak, T. Szoplik, Photonic Crystal: Physics and Technology, Spinger-Verlag, Italia, 2008.
[21] J.M. Lourtioz, Photonic Crystal, Spinger-Verlag, Berlin, 2008.
[22] J. Jasieniak, et al., Sol–gel based vertical optical microcavities with quantum dot defect layers, Adv. Funct. Mater. 18 (2008) 3772.
[23] L.C. Klein, G.J. Garvey, Kinetics of the sol–gel transition, J. Non-Cryst. Solids 38 (1980) 45.
[24] C.J. Brinker, K.D. Keefer, D.W. Schaefer, R.A. Assink, B.D. Kay, C.S. Ashley, Sol–gel transition in simple silicates, J. Non-Cryst. Solids 48 (1982) 47.
[25] T. Olding, M. Sayer, D. Barrow, Ceramic sol–gel composite coatings for electrical insulation, Thin Solid Films 398–399 (2001) 581–586.
[26] T. Troczynski, Q. Yang, Process for making chemically bonded sol-gel ceramics. US Patent No. 6,284,682, 2001.
[27] T. O'Haver, Worksheets for Analytical Calibration Curves, The University of Maryland, 2013 http://terpconnect.umd.edu/ toh/models/CalibrationCurve.html

Biographies

Mamat Rahmat is currently a faculty member at the Department of Physics, Bogor Agricultural University, Indonesia. He obtained his B.S. in Physics in 2000 and M.S. in Bio-physics in 2010 both from Bogor Agricultural University, Indonesia. He is also member of Indonesian Optical Society (InOS). His research interests include photonic crystal, sensor, electronic, instrumentation, and software development.

Wenny Maulina has been graduated as Master Degree at Biophysics Program, Graduate School, Bogor Agricultural University. She received a BS degree in Physics from the same university in 2008. Her research interests are biosensor, photonic crystal, and membrane.

Isnaeni has been working as post-doctoral researcher at Department of Physics, KAIST, Korea since 2012. He received his B.Sc. from Bogor Agricultural University, Indonesia in 2000, his M.Sc. from The University of Queensland in 2006, and his Ph.D. from Korea Advanced Institute of Science and Technology, Korea in 2012. His research interest is on photonic crystals, metal nanoparticles, and low dimensional semiconductor nanophotonics, such as quantum dots, nanowires, and nanorods.

Dede Yulias Nurul Miftah has been graduated as Bachelor Degree at Physics Program, Faculty of Mathematics and Natural Science, Bogor Agricultural University. His research interests include photonic crystal, sensor, electronic, and instrumentation.

Nissa Sukmawati has been graduated as Bachelor Degree at Physics Program, Faculty of Mathematics and Natural Science, Bogor Agricultural University. Her research interests are include photonic crystal, and gas sensor.

Erus Rustami has been graduated as Master Degree at Biophysics Program, Graduate School, Bogor Agricultural University. He received a BS degree in Physics from the same university in 2008. He is also member of Indonesian Optical Society (InOS). His research interests are include electronic, instrumentation, and software development.

Muhamad Azis has been graduated as Master Degree at Biophysics Program, Graduate School, Bogor Agricultural University. He received a BS degree in Physics from the same university in 2008. His research interests are include electronic, instrumentation, and embedded system

Kudang Boro Seminar is a Professor in Computer Technology in the Department of Mechanical and Biosystem Engineering, Bogor Agricultural University (IPB), Indonesia. He received M.Sc. and Ph.D. in Computer Science from University of New Brunswick, Canada. He is a board member of AFITA (Asean Federation for Information Technology in Agriculture) & ISAI (Indonesian Society of Agriculture Informatics). His research interests include Information Engineering, Software Engineering, Intelligent System, Distance Learning, Internetworking, Computer Based Instrumentation and Control system.

Arief Sabdo Yuwono is an Associate Professor in the Department of Civil and Environmental Engineering, Bogor Agricultural University. He received BS degree in Agricultural Engineering from Bogor Agricultural University, Indonesia, in 1989, MSc in Environmental Sanitation from University of Gent, Belgium, in 1996, and PhD degree in Bio-Environmental Engineering from University of Bonn, Germany, in 2003. His research interests include environmental monitoring, environmental instrumentation, water and air pollution quality control. He was an air quality and noise expert, air emission expert, and environmental and agricultural specialist.

Yong-Hoon Cho is a professor at Department of Physics, KAIST, Korea. Since 2010, he has been in charge of KAIST Center for LED Research. He received his B.Sc. degree in physics from Sogang University in 1989, and the M.Sc. and Ph.D. degrees in solid state physics from Department of Physics, Seoul National University in 1992 and 1997, respectively. He is currently a reviewer of Applied Physics Letters/Journal of Applied Physics/Journal of Korean Physical Society and a member of KPS, APS, AIP, MRS, OSA, SPIE, KSEA, and AKPA. His current research interests are growth, fabrication, and various structural, electrical, and optical characterizations of micro- and nano-scale III–V compound optoelectronic semiconductor quantum structures.

Husin Alatas is an Associate Professor in Department of Physics, Bogor Agricultural University, Indonesia. He received BS, M.Sc, and PhD degree from Institut Teknologi Bandung, Indonesia, in 1995, 1998, and 2005, respectively. Currently, he is Head of Theoretical Physics Division at Bogor Agricultural University. He is also member of the Indonesian Optical Society (InOS), and Optical Society of America (OSA). His research interests include the theory and modeling of photonic crystal based sensor.